ACS APPLIED MATERIALS & INTERFACES

Research Article

www.acsami.org

Multi-Functional Envelope-Type Nanoparticles Assembled from Amphiphilic Peptidic Prodrug with Improved Anti-Tumor Activity

Jing-Xiao Chen,[†,‡,§] Xiao-Ding Xu,[†,§] Wei-Hai Chen,[†] and Xian-Zheng Zhang*[,†]

[†]Key Laboratory of Biomedical Polymers of Ministry of Education, Department of Chemistry, Wuhan University, Wuhan 430072, P. R. China

[‡]School of Pharmaceutical Science, Jiangnan University, Wuxi 214122, P. R. China

Supporting Information

ABSTRACT: A novel multifunctional amphiphilic peptidic prodrug was reported here by conjugating the antitumor drug of doxorubicin (DOX) to the hydrophobic tail of a designed peptide-amphiphile (PA), in which the hydrophilic peptide headgroup comprises a glycine-arginine-glycine-aspartic acid-serine (GRGDS) sequence and octaarginine (R_8) sequence. Because of the amphiphilic nature, this peptidic prodrug can spontaneously self-assemble into spherical multifunctional envelop-type nanoparticles (MENPs) with the functional peptide sequences gathered on surface. By means of the multifunctions of RGD-mediated tumor targeting, R_8-mediated membrane penetration and intracellular protease-mediated hydrolyzing peptide bonds, the MENPs could targeted deliver doxorubicin (DOX) to tumor cells, showing improved antitumor activity both in vitro and in vivo with much reduced side effects.

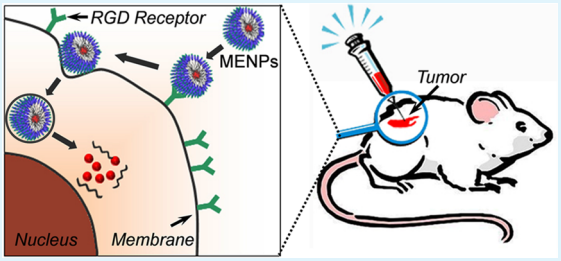

KEYWORDS: *peptidic prodrug, multifunctional envelope-type nanoparticle, RGD, antitumor*

1. INTRODUCTION

Nanoparticles (NPs) have emerged as a promising tool to deliver drugs for the treatment of cancer.[1−3] In the field of cancer chemotherapy, NPs and nanomedicines have achieved encouraging results in clinical/preclinical treatment, such as prolonged blood circulation time and promoted targeting effect.[4,5] However, there still exist some intractable problems for the application of NPs.[6−8] For example, the premature drug leakage, burst release during blood circulation, the drug-loading efficiency varying with the change in the batch of NPs and lack of targeting activity to cause undesired toxic side effects. To overcome these drawbacks, a promising strategy is to conjugate the antitumor drugs to (macro)molecules to construct prodrugs that can be metabolized in vivo into active metabolites.[9−13] Kopecek et al. have reported various kinds of polymer−doxorubicin conjugates for drug delivery, some of which have achieved favorable results in tumor inhibition and overcoming multidrug resistance.[14−16] Additionally, current design also focuses on the development of tissue specificity via covalently linking the prodrugs to tumor-targeting ligands, such as aptamers, antibodies, and peptides.[17−20] However, the stability of the ligands is another tough nut because of the rapid enzymatic degradation in vivo.[21]

Recently, peptidic NPs that self-assemble by peptide-amphiphiles (PAs) have shown distinct advantages for the use as drug carriers. At first, peptidic NPs provide a multivalent display of PAs,[22,23] and thus can protect peptide sequences from degradation to some extent.[24−26] Second, peptidic NPs with various sizes and shapes can be formed by adjusting the hydrophilic/hydrophobic balance of PAs.[27−29] Many recent reports have demonstrated that the size and shape of NPs can affect their biological behaviors such as membrane penetration and immune response.[30−32] It is known that many small peptides have unique bioactivities such as targeting tumors and penetrating cell membrane,[33−36] one may therefore construct PA-based prodrugs to from multifunctional envelope-type nanoparticles (MENPs). Thus, various small peptides sequences with different activities can be packaged into a single system and work reasonably, timely and locally according to the predetermined strategy.[37,38] Additionally, with the aid of the hydrophobic antitumor drugs to adjust the molecular self-assembly,[39−42] the peptide sequences can be gathered on the surface of aggregates, which not only protect them from degradation to some extent but realize the convergence of various biological activities to strengthen the antitumor activity.[25,26]

Herein, we reported a novel concept of multifunctional amphiphilic peptidic prodrug. The prodrug was obtained by conjugating doxorubicin (DOX) as the model drug to the hydrophobic tail of a designed PA (Scheme 1). The peptide headgroup, which comprises a glycine-arginine-glycine-aspartic acid-serine (GRGDS) sequence and octaarginine (R_8) sequence, not only improves the water solubility of DOX but endows the prodrug with tumor-targeting and membrane-penetrating activities.[33−36] More importantly, because of the amphiphilic nature, this prodrug can spontaneously self-

Received: October 22, 2013
Accepted: December 15, 2013
Published: December 15, 2013

Scheme 1. Schematic Illustration of (A) MENPs Self-Assembly of PA-DOX and (B) the Targeted Release of DOX in Tumor Cells[a]

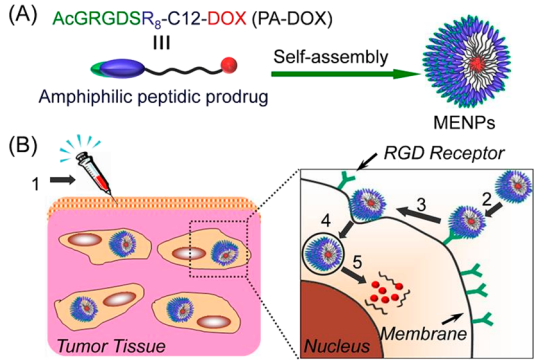

[a]After (1) injection around tumor tissue, (2, 3) the RGD-mediated endocytosis and R8-mediated membrane penetration leads to (4) the uptake of the MENPs by endosome/lysosome of tumor cells. Subsequently, (5) the intracellular proteases hydrolyze the peptide bonds of PA-DOX and thus induce the rapid release of DOX, presenting anti-tumor activity in vivo.

assemble into stable MENPs with DOX encapsulated in the hydrophobic core and functional peptide sequences gathered on the shell. The obtained MENPs could make use of their multifunctions (i.e., RGD-mediated targeting, R_8-mediated membrane penetration and protease-triggered DOX release) to deliver DOX into tumor cells, showing improved antitumor activity and much reduced side effects of DOX both in vitro and in vivo.

2. EXPERIMENTAL SECTION

2.1. Materials. *N*-Fluorenyl-9-methoxycarbonyl (FMOC) protected *L*-amino acids (FMOC-Gly-OH, FMOC-Asp(OtBu)−OH, FMOC-Arg(Pbf)−OH, FMOC-Ser(tBu)−OH) and 2-chlorotrityl chloride resin (100−200 mesh, loading: 0.4 mmol/g) were purchased from GL Biochem (Shanghai) Ltd. (China) and used as received. 1-Hydroxybenzotriazole (HOBt), trifluoroacetic acid (TFA), *o*-benzotriazole-*N*,*N*,*N*′,*N*′-tetramethyluroniumhexafluorophosphate (HBTU), piperidine, acetic acid, 9-fluorenylmethoxy carbonyl chloride (FMOC-Cl), benzotriazol-1-yloxytripyrrolidinophosphonium hexafluorophosphate (PyBOP), 1,2-ethanedithiol (EDT), dioxane and phenol were provided by Shanghai Reagent Chemical Co. (China) and used directly. Doxorubicin hydrochloride (DOX·HCl) was purchased from Zhejiang Hisun Pharmaceutical Co. (China) and used as received. Dimethylformamide (DMF), dichloromethane (DCM), and diisopropylethylamine (DiEA) were obtained from Shanghai Reagent Chemical Co. (China) and distilled prior to use. Thioanisole, triisopropylsilane (TIS) and 12-aminododecanoic acid (NH_2-C11-COOH) were purchased from ACROS (USA) and used without further purification. Dulbecco's Modified Eagle's Medium (DMEM), fetal bovine serum (FBS), molecular probe (Hoechst 33258), 3-[4,5-dimethylthiazol-2-yl]-2,5-diphenyltetrazoliumbromide (MTT), trypsin and penicillinestreptomycin were purchased from Invitrogen Corp. All other reagents and solvents were of analytical grade and used directly. Cathepsin B (2.73×10^6 U/g, bovine spleen) was donated by Biology Institute, Guangxi Academy of Sciences (China).

2.2. Synthesis of FMOC-C11-COOH. The amino group of NH_2-C11-COOH was protected by 9-fluorenylmethyloxycarbonyl (FMOC) group according to our recent report.[36] In brief, NH_2-C11-COOH (4.31 g, 20 mmol) was suspended in a mixed solution of dioxane (20 mL) and Na_2CO_3 aqueous solution (10 wt %, 100 mL) and then cooled in an ice bath. Subsequently, a solution of FMOC-Cl (5.18 g, 20 mmol) in dioxane (40 mL) was added with stirring. The mixture was allowed to stir at room temperature for 6 h. The dioxane was then removed by rotary evaporation and 250 mL of distilled water was added. Thereafter, the aqueous solution was acidified to a pH of 3 with concentrated HCl and the product was extracted by ethyl acetate. After drying over anhydrous $MgSO_4$, the crude product was collected by removing solvent. The purification was carried out via the recrystallization from acetonitrile. ^{1}H NMR, 300 MHz, DMSO-d6 (ppm): 11.96 (s, 1H), 7.10−7.90 (m, 8H), 6.74 (s, 1H), 4.10−4.37 (m, 3H), 2.94 (t, 2H), 2.13(t, 2H), 1.10−1.50 (m, 18H). The ^{1}H NMR spectrum is shown in Figure S1 in the Supporting Information.

2.3. Synthesis of Fully Protected PA. The fully protected PA ($AcGRGDSR_8$-C11-COOH) was synthesized manually on the 2-chlorotrityl chloride resin employing a standard FMOC solid phase peptide synthesis (SPPS) technique. Before the reaction, the resin was washed with DCM and DMF for 3 times respectively, and then immersed in DMF for 30 min. After draining off, a DMF solution of the mixture of FMOC-C11-COOH (4 equiv relative to resin loading) and DiEA (6 equiv) was added to the resin and shaken for 0.5 h at room temperature. After removing the reaction solution, the resin was washed with DMF (three times). Subsequently, 20% piperidine/DMF (v/v) solution was introduced to the resin to remove the FMOC protected groups. After shaking for 20 min, the reaction solution was drained off and the resin was washed with DMF (three times). The presence of free amino groups was indicated by a blue color in the Kaiser test. Thereafter, a DMF solution of the mixture of FMOC protected amino acid (4 equiv), HBTU (4 equiv), HOBt (4 equiv) and DiEA (6 equiv) was added. After shaking at room temperature for 1.5 h, the reaction solution was drained off and the resin was washed with DMF (three times). The absence of free amino groups was indicated by a yellow color in the Kaiser test. After the repetition of deprotection and acylation reaction to obtain the peptide sequence, the *N*-terminus of the peptide sequence was capped with acetyl group through the addition of the mixture of acetic acid (4 equiv), HBTU (4 equiv), HOBt (4 equiv), and DiEA (6 equiv). Thereafter, the resin was washed with DMF (three times) and DCM (three times). Cleavage of the fully protected peptide from the resin was performed using a mixture of 0.5% TFA, 2.5% TIS, and 97% DCM. After cleavage for ten times (10 mL × 10 min), the cleavage mixture and DCM washing were collected. After the addition of trimethylamine to neutralize the residual TFA, the cleavage mixture was concentrated to a viscous solution by rotary evaporation. The product was collected after precipitation in cold ether for three times and subsequently dried under vacuum.

2.4. Synthesis of PA-DOX. The fully protected peptide (1 g, 0.23 mmol), PyBOP (0.18 g, 0.35 mmol) and HOBt (0.05 g, 0.35 mmol) were dissolved in 20 mL of dry DMF. After activating the terminal carboxyl acid group of the fully protected peptide for 30 min, 20 mL of DMF solution containing DOX·HCl (0.16 g, 0.28 mmol) and DiEA (1.5 mL, 9.2 mmol) was added. After the reaction in dark for 24 h, the solvent of DMF was removed under reduced pressure and the crude product was purified on a silica gel column, eluting with methanol/DCM (1/7). The synthesis route and ^{1}H NMR spectrum of the fully protected prodrug are respectively shown in Figures S2 and S3 (Supporting Information). To remove the protected group, the fully protected prodrug was dissolved in a mixture of 83% TFA, 6.3% phenol, 4.3% thioanisole, 4.3% H_2O, and 2.1% EDT. After stirring for 2 h, the solution was concentrated and cold ether was added to precipitate the crude product. After purification through HPLC with a C18 column and using a linear gradient of acetonitrile and DI water containing 0.1% TFA, the expected amphiphilic peptidic prodrug of PA-DOX ($AcGRGDSR_8$-C12-DOX) was collected.

2.5. Preparation and Characterizations of MENPs. The MENPs of PA-DOX were prepared by directly dissolving the amphiphilic peptidic prodrug in deionized water (pH 7.0) and subsequently placing for 30 min in dark. The morphology of the MENPs was observed on a Tecnai G20 S-TWIN transmission electron microscope (TEM) with an acceleration voltage of 200 kV. Before observation, the aqueous solution of the MENPs (0.1 mg/mL) was applied to a copper grid and dried in air. The size distribution and ζ-potential of the MENPs were determined using dynamic light

scattering (DLS) techniques with a Nano-ZS ZEN3600 instrument (MALVERN Instruments).

2.6. In Vitro Enzymatic Release of DOX. The MENPs of PA-DOX (3 mg), in which the amount of total peptide bonds is around 18 μmol, was dispersed in 3 mL of PBS (0.1 M, pH 7.4) solution and 20 U cathepsin B was added. After the enzymatic hydrolysis of peptide bonds for 15 min at physiological temperature (37 °C), the solution was transferred to a dialysis tube (MWCO 1000 Da) and then subjected to dialysis against 10 mL of PBS at 37 °C. At a predetermined time interval, all of the PBS solution was withdrawn and another 10 mL of fresh PBS was added after each sampling. The amount of DOX released from the MENPs was measured by using a UV spectrophotometer (Perkin-Elmer Lambda Bio 40 UV/vis spectrometer, USA) at 497 nm. The average value of three independent experiments was collected and the cumulative DOX release was calculated as follows: Cumulative DOX release (%) = (M_t / M_∞) × 100, where M_t is the amount of DOX release from the MENPs and M_∞ is the amount of conjugated DOX in PA-DOX.

2.7. Cell Culture. Human cervix carcinoma (HeLa) and transformed African green monkey SV40-transformed kidney fibroblast (COS7) cell-lines were respectively incubated in DMEM medium with 10% FBS and 1% antibiotics (penicillin-streptomycin, 10,000 U/mL) at 37 °C in a humidified atmosphere containing 5% CO_2.

2.8. In Vitro Cytotoxicity Assay. The cytotoxicity assay was performed against HeLa and COS7 cell-lines by MTT assay. In brief, HeLa and COS7 cells were harvested and seeded in a 96-well plate with a density of 6000 cells/well. After the incubation in 100 μL of DMEM containing 10% FBS for 24 h, a assigned amount of PA-DOX dissolved in 200 μL of DMEM was added and the cells were allowed to incubate for another 48 h. DOX solution with containing 5% (v/v) DMSO as the cosolvent was used as the positive control. After replacing the medium with 200 μL of fresh DMEM, 20 μL of MTT (5 mg/mL in PBS) solution was added to each well and the cells were further incubated for 4 h. Subsequently, the medium was removed and 150 μL of DMSO was added. After shaking at room temperature for several minutes, the optical density (OD) was measured at 570 nm with a microplate reader model 550 (Bio-Rad, USA). The average value of four independent experiments was collected and the cell viability was calculated as follows: Cell viability (%) = (OD_{sample}/ $OD_{control}$) × 100, where $OD_{control}$ is obtained in the absence of PA-DOX and OD_{sample} is obtained in the presence of PA-DOX.

2.9. Intracellular Uptake. The HeLa and COS7 cells were respectively seeded in 6-well plates and incubated in 1 mL of DMEM containing 10% FBS for 24 h. Subsequently, the MENPs of PA-DOX dispersed in DMEM (0.1 mg/mL) were added and the cells were allowed to incubate for another 4 h. Then the nuclei were stained by blue molecular probe Hoechst 33258 (10 mg/mL in water stock solution) for 15 min. After removing the medium and subsequently washing with PBS buffer for several times, the stained cells were viewed under a confocal laser scanning microscope (Nikon C1-si TE2000, Japan) with the excitation at 408 nm for blue molecular probe and 488 nm for DOX.

2.10. Construction of Tumor-Bearing Nude Mice. Healthy female BALB/c nude mice (4−5 weeks old, 18−22 g) were purchased from Wuhan University experimental animal center/Animal Biosafety Level 3 Laboratory (ABSL-3 lab) (Wuhan, China). The animal tumor model was generated by subcutaneous injection with 0.1 mL of HeLa cell suspension with a density of 1 × 10^7 cells/mL into the forelimb armpit region of nude mice. After a month, the length of the HeLa tumor xenograft reached about 7−8 mm, then the mice were sacrificed by cervical vertebra dislocation and the tumors were harvested. Subsequently, the tumors were cut into pieces, crushed into homogenate and finally made into cell suspension with a density 1 × 10^7 cells/mL. Then, 0.1 mL of this cell suspension was injected to the back region of nude mice. Around 5 days later, the tumor-bearing nude mice with a tumor length of 4−5 mm were collected to use for the evaluation the antitumor activity of the MENPs of PA-DOX. All animal procedures were in accordance with the guidelines of the Institutional Animal Care and Use Committee.

2.11. In Vivo Antitumor Evaluation. Four randomly divided groups of tumor-bearing nude mice (n = 6) were used to evaluate the in vivo antitumor activity.[43,44] In the first group, the mice were treated once every day at a dose of 5 mg of free DOX per kg of mouse body weight (5 mg/kg DOX group) through subcutaneous injection as the positive control. In the second and third group, the mice were treated once every day at a respective dose of 20 mg (20 mg/kg MENPs group) and 50 mg (50 mg/kg MENPs group) MENPs of PA-DOX per kg of mouse body weight through subcutaneous injection. In the fourth group, PBS was subcutaneously injected to tumor-bearing nude mice every day as the negative control (PBS group). The tumor growth was monitored every one day by measuring perpendicular diameters using a caliper and tumor volume that calculated as follows: $V = W^2L/2$, where W and L are the shortest and longest diameters, respectively. After the continuous treatment for 20 days, the mice were sacrificed by cervical vertebra dislocation and the tumors were immediately harvested, weighed and histologically analyzed.

3. RESULTS AND DISCUSSION

3.1. Synthesis of the Peptidic Prodrug. Starting from the *N*-fluorenyl-9-methoxycarbonyl (FMOC) protected 12-amino-dodecanoic acid, we first synthesized the fully protected PA (AcGRGDSR$_8$-C11-COOH) via standard FMOC chemistry. After conjugating DOX to the hydrophobic tail of PA and purifying the crude product, the multifunctional amphiphilic peptidic prodrug (AcGRGDSR$_8$-C12-DOX, PA-DOX) was collected. The molecular weight of PA-DOX found in electrospray ionization-mass spectrometry (ESI-MS) spectrum was 836.4 $[M+3H]^{3+}$ (calcd M_w: 2504.8).

3.2. Characterizations of the MENPs. Due to the amphiphilic nature of PA-DOX, the MENPs of this peptidic prodrug were prepared via the self-assembly of PA-DOX in aqueous solution. From the TEM image revealed in Figure 1A,

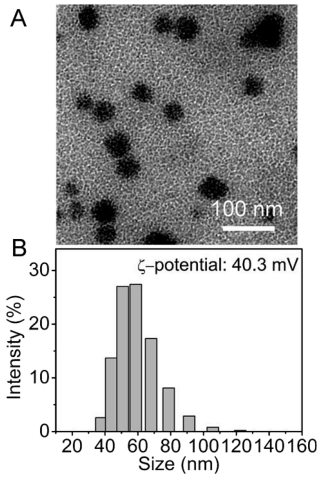

Figure 1. (A) TEM image and (B) size distribution and ζ-potential measurements of the MENPs of PA-DOX (0.1 mg/mL in pH 7.4 PBS solution) in aqueous medium.

PA-DOX at a concentration of 0.1 mg/mL can self-assemble into well-dispersed spherical MENPs. The average diameter estimated from TEM image was about 50 nm, which was close to the result of DLS measurement of 88.7 nm (±2.3 nm), as shown in Figure 1B. The size and size distribution of these self-assembled MENPs are reproducible, with three independent preparations giving nearly identical result for each sample. The measured ζ-potential was 40.3 mV, which indicated the MENPs were stable in aqueous medium. It is particularly noted that the strategy of prodrug self-assembly allows the preparation of

MENPs with the same drug-loading level to reach a high value of around 21.7 wt %. This result is a significant improvement on traditional drug-loaded NPs, which usually carry drug payloads of only a few percent.

3.3. In Vitro Enzymatic Drug Release. To demonstrate that the conjugated DOX can be released from the MENPs in the presence of proteases, cathepsin B, a commercial proteolytic enzyme that can specifically hydrolyze the peptide bonds was added. As shown in Figure 2, the MENPs of PA-DOX show a

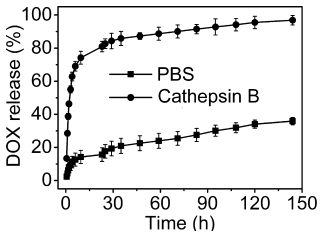

Figure 2. In vitro drug release behavior of the MENPs of PA-DOX (0.1 mg/mL in pH 7.4 PBS) at physiological temperature (37 °C) with the addition of 20 U cathepsin B.

rapid release behavior with the addition of cathepsin B and around 75% conjugated DOX is released out within 10 h. As a control, lower than 35% conjugated DOX is released within 144 h without cathepsin B. On the basis of this encouraging result, we believe that the peptide bonds of the MENPs of PA-DOX could be also intracellularly hydrolyzed to release DOX as there are numerous types of proteases in tumor cells with various functions.[45,46]

3.4. Cellular Uptake. To demonstrate that the MENPs could use their multifunctions to specifically target tumor cells and induce cell apoptosis, we chose the cell-lines of HeLa (cervical cancer cells) and COS7 (African green monkey SV40-transformed kidney fibroblast cells) and respectively incubated with the MENPs. From the confocal laser scanning microscopy (CLSM) images revealed in Figure 3, the red color corresponding to the fluorescence of DOX distributes on the whole cytoplasma, indicating that the MENPs have been uptaken by HeLa cells after incubation for 4 h (Figure 3A). Through staining the nuclei with blue molecular probe, it can be found that a number of the MENPs accumulate in the nuclei. Moreover, some cells become collapsed with cell morphology changing from elongated shape to spherical shape. Since DOX is encapsulated in the inner core of the MENPs, this result strongly demonstrates that the peptide bonds of the MENPs can be hydrolyzed by the intracellular proteases to release cytotoxic DOX. In contrast, the amount of the MENPs uptaken by COS7 cells is rather lower in comparison with HeLa cells, as demonstrated by the weak red fluorescence presented in Figure 3B. The reason is that the overexpressed integrins of $\alpha_v\beta_3$ and $\alpha_v\beta_5$ on the tumor cells facilitate the efficient recognition of the RGD ligands distributed on the surface of the MENPs,[31−33] leading to a dramatically increased cellular uptake.

3.5. In Vitro Cytotoxicity Assay. The in vitro cytotoxicity of PA-DOX against HeLa and COS7 cells was further assessed by MTT assay. As shown in Figure 3C, due to the absence of cell specificity, there is no prominent difference in the half maximal inhibitory concentration (IC50) of free DOX against HeLa (2.47 mg/L) and COS7 (1.79 mg/L) cells. However, after conjugation to the PA, the IC50 of PA-DOX against these

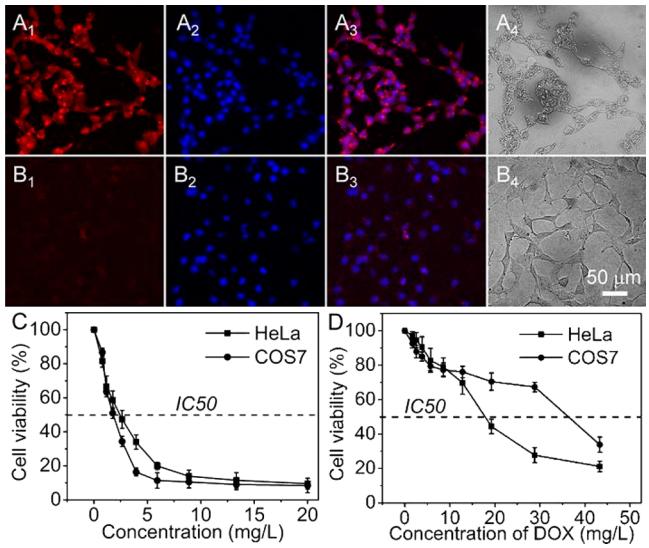

Figure 3. CLSM images of (A) HeLa and (B) COS7 cells incubated with the MENPs (0.1 mg/mL) for 4 h, and the viability of HeLa and COS7 cells incubated with (C) free DOX and (D) the PA-DOX at different concentrations for 48 h. (A_1, A_2, B_1, B_2) confocal fluorescence images; (A_3) confocal fluorescence image overlay of A_1 and A_2; (B_3) confocal fluorescence image overlay of B_1 and B_2; (A_4, B_4) bright-field images.

two cell lines shows a significant difference (Figure 3D) and the corresponding IC50 values respectively increase to 81.9 (equivalent to 17.8 mg/L free DOX) and 167.9 mg/L (equivalent to 36.4 mg/L free DOX). Although the construction of multifunctional peptidic prodrug induces the decline in the cytotoxicity of DOX, the incorporation of functional peptide sequences can significantly improve the selectivity of DOX to tumor cells, implying a great potential for application of the MENPs for antitumor in vivo.

3.6. In Vivo Antitumor Evaluation. The in vivo antitumor activity of the MENPs was evaluated against the human cervical tumor xenograft model in nude mice. The tumor-bearing mice were randomly divided into four groups (n = 6) and respectively treated with PBS, 5 mg/kg free DOX, and 20 and 50 mg/kg MENPs of PA-DOX through a single subcutaneous injection once every day. As exhibited in Figure 4A, without any treatment, the xenografted tumor volume of PBS group rapidly increases to 438.3 mm^3 20 days later. Although the tumor growth rate is lower than that in PBS group, the tumor volume in the 20 mg/kg MENPs group still increases to 319.1 mm^3 within the same time frame. However, increasing the injection dose of MENPs to 50 mg/kg can significantly inhibit the tumor growth and the relative xenografted tumor volume decreases to around 11.1 mm^3 after the treatment for 20 days. This result is in good agreement with the tumor weight in these three groups. As presented in Figure 4B, after treatment for 20 days, the tumor weight in 50 mg/kg MENPs group is around 5.5 mg, which is rather lower than that in PBS (~300.9 mg) and 20 mg/kg MENPs (~116.5 mg) groups. Although free DOX can also achieve the equivalent antitumor effect (around 15.3 mm^3 in tumor volume and 6.1 mg in tumor weight 14 days later) as that in 50 mg/kg MENPs group, the use of free DOX induces severely toxic side effects. From the images in Figure 4C, injection of free DOX for 12 days leads to the skin ulcer. However, due to the tumor targeting and protease-triggered

dx.doi.org/10.1021/am404680n | ACS Appl. Mater. Interfaces 2014, 6, 593−598

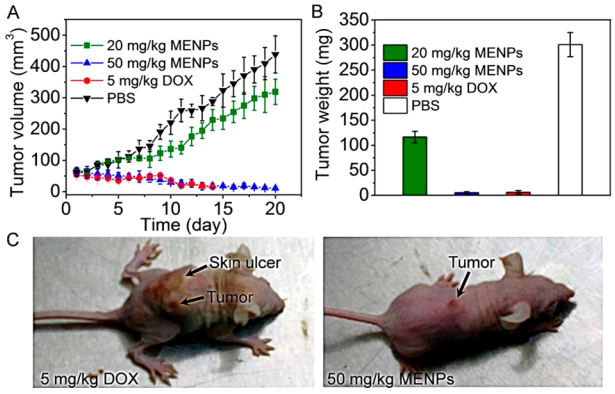

Figure 4. (A) Tumor volume and (B) weight of human cervical tumor xenografted nude mice in PBS, 5 mg/kg DOX, 20 mg/kg MENPs, and 50 mg/kg MENPs groups. (C) Photo images of the tumor xenografted nude mice treated with free DOX and MENPs of PA-DOX for 12 days at a respective dose of 5 and 50 mg per kg of mouse body weight.

release of DOX from the MENPs, the skin of the mice is smooth and no ulcer can be observed. This result is of great importance as it strongly demonstrates that the MENPs of PA-DOX can significantly inhibit tumor growth with the alleviation of toxic side effects.

3.7. Histological Examination. We further used histological examination to analyze the antitumor activity of the MENPs of PA-DOX. As displayed in Figure 5, the tumors

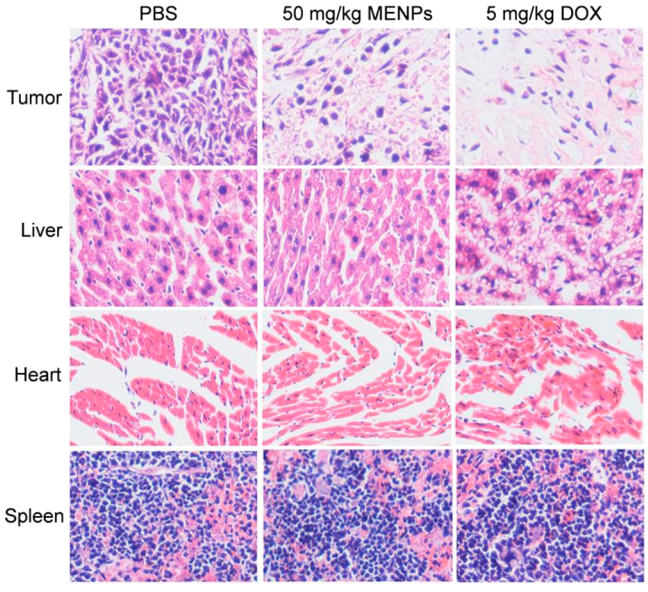

Figure 5. Histological section of the tumor, liver, heart, and spleen tissues of the mice after the respective treatment with PBS, MENPs of PA-DOX, and free DOX. Hematoxylin-eosin; magnification 200× .

treated with PBS are typically made up of abundant tumor cells and no obvious damage can be observed. However, the extensive apoptotic cells and a large area of dead cells without nuclei are observed in the MENPs of PA-DOX and free DOX treated tumors, indicating that the MENPs of PA-DOX show the equivalent therapeutic effect as the free DOX. However, because the MENPs can use their multifunctions especially the tumor-targeting function, the administration of the MENPs does not induce the subacute toxicity including hepatotoxicity and cardiotoxicity that are usually encountered in the free DOX-mediated treatment.[43,44] The morphology of the cells in liver and heart tissues is similar as that treated with PBS and only a few apoptotic cells can be found. In contrast, the injection of free DOX leads to a prominent hepatotoxicity, such as large number of vacuoles within liver cells, extensive nuclear shrinkage and apoptotic liver cells. And also, the severe myocardial damage can be observed in the mice treated with free DOX, as demonstrated by the disordered arrangement of myocardial cells and the shrinkage of some myocardial cells. It should be noted that there is no obvious toxicity for free DOX and the MENPs of PA-DOX in the organ of spleen. Anyway, the toxicity to liver and heart, especially the irreversible cardiotoxicity, are the principal reason to induce the mice death in the free-DOX-treated group.[43,44]

4. CONCLUSIONS

In conclusion, we reported a novel multifunctional amphiphilic peptidic prodrug of PA-DOX by conjugating the antitumor drug, DOX to the hydrophobic tail of amphiphilic peptide with tumor-targeting and membrane-penetrating functions. Due to the amphiphilic nature, this peptidic prodrug can spontaneously self-assemble into stable MENPs with DOX encapsulated in the hydrophobic inner core and the functional peptide sequences of RGDS and R_8 gathered on outer shell. By using the multifunctions of RGD-mediated tumor targeting, R_8-mediated membrane penetration and intracellular protease-mediated hydrolyzing peptide bonds, the MENPs could targetedly transport and release DOX to tumor cells, presenting improved antitumor activity with much reduced side effects. The novel concept of peptidic prodrug demonstrated here may open a window to develop other peptidic prodrugs for cancer therapy.

■ ASSOCIATED CONTENT

Ⓢ Supporting Information

Additional figures of synthesis route and ^{1}H NMR spectra. This material is available free of charge via the Internet at http://pubs.acs.org.

■ AUTHOR INFORMATION

Corresponding Author

*E-mail: xz-zhang@whu.edu.cn. Tel.: + 86 27 6875 5993. Fax: + 86 27 6875 4509.

Author Contributions

§Authors J.-X.C. and X.-D.X. contributed equally.

Notes

The authors declare no competing financial interest.

■ ACKNOWLEDGMENTS

This work was supported by National Key Basic Research Program of China (2011CB606202), the Ministry of Education of China (20120141130003), and National Natural Science Foundation of China (51125014, 51233003 and 21204068).

■ REFERENCES

(1) Brigger, I.; Dubernet, C.; Couvreur, P. *Adv. Drug Delivery Rev.* **2002**, *54*, 631−651.
(2) Ferrari, M. *Nat. Rev. Cancer* **2005**, *5*, 161−171.
(3) Barreto, J. A.; O'Malley, W.; Kubeil, M.; Graham, B.; Stephan, H.; Spiccia, L. *Adv. Mater.* **2011**, *23*, H18−H40.
(4) Ulbrich, K.; Subr, V. *Adv. Drug Delivery Rev.* **2004**, *56*, 1023−1050.
(5) Kamaly, N.; Xiao, Z.; Valencia, P. M.; Radovic-Moreno, A. F.; Farokhzad, O. C. *Chem. Soc. Rev.* **2012**, *41*, 2971−3010.

(6) Kang, N.; Perron, M. E.; Prud'homme, R. E.; Zhang, Y.; Gaucher, G.; Leroux, J. C. *Nano Lett.* **2005**, *5*, 315−319.
(7) Rapoport, N. *Prog. Polym. Sci.* **2007**, *32*, 962−990.
(8) Wang, W.; Cheng, D.; Gong, F.; Miao, X.; Shuai, X. *Adv. Mater.* **2012**, *24*, 115−120.
(9) Albert, A. *Nature* **1958**, *182*, 421−423.
(10) Han, H. K.; Amidon, G. L. *AAPS Pharm. Sci.* **2000**, *2*, 48−58.
(11) Khandare, J.; Minko, T. *Prog. Polym. Sci.* **2006**, *31*, 359−397.
(12) Rautio, J.; Kumpulainen, H.; Heimbach, T.; Oliyai, R.; Oh, D.; Jarvinen, T.; Savolainen, J. *Nat. Rev. Drug Discovery* **2008**, *7*, 255−270.
(13) Mahato, R.; Tai, W.; Cheng, K. *Adv. Drug Delivery Rev.* **2011**, *63*, 659−670.
(14) Omelyanenko, V.; Kopeckova, P.; Gentry, C.; Kopecek, J. *J. Controlled Release* **1998**, *53*, 25−37.
(15) Minko, T.; Kopeckova, P.; Kopecek, J. *J. Controlled Release* **1999**, *59*, 133−148.
(16) Nori, A.; Kopecek, J. *Adv Drug Delivery Rev.* **2005**, *57*, 609−636.
(17) Chen, X.; Plasencia, C.; Hou, Y.; Neamati, N. *J. Med. Chem.* **2005**, *48*, 1098−1106.
(18) Quiles, S.; Raisch, K. P.; Sanford, L. L.; Bonner, J. A.; Safavy, A. *J. Med. Chem.* **2010**, *53*, 586−594.
(19) Tai, W.; Mahato, R.; Cheng, K. *J. Controlled Release* **2010**, *146*, 264−275.
(20) Kolishettia, N.; Dhar, S.; Valencia, P. M.; Lin, L. Q.; Karnik, R.; Lippard, S. J.; Langer, R.; Farokhzad, O. C. *Proc. Natl. Acad. Sci. U.S.A.* **2010**, *107*, 17939−17944.
(21) Singh, Y.; Palombo, M.; Sinko, P. J. *Curr. Med. Chem.* **2008**, *15*, 1802−1826.
(22) Hartgerink, J. D.; Beniash, E.; Stupp, S. I. *Science* **2001**, *294*, 1684−1688.
(23) Boato, F.; Thomas, R. M. M.; Ghasparian, A.; Freund-Renard, A.; Moehle, K.; Robinson, J. A. *Angew. Chem., Int. Ed.* **2007**, *46*, 9015−9018.
(24) Lee, K. C.; Carlson, P. A.; Goldstein, A. S.; Yager, P.; Gelb, M. H. *Langmuir* **1999**, *15*, 5500−5508.
(25) Missirlis, D.; Khant, H.; Tirrell, M. *Biochemistry* **2009**, *48*, 3304−3314.
(26) Soukasene, S.; Toft, D. J.; Moyer, T. J.; Lu, H.; Lee, H. K.; Standley, S. M.; Cryns, V. L.; Stupp, S. I. *ACS Nano* **2011**, *5*, 9113−9121.
(27) Tsonchev, S.; Niece, K. L.; Schatz, G. C.; Ratner, M. A.; Stupp, S. I. *J. Phys. Chem. B* **2008**, *112*, 441−447.
(28) Jin, Y.; Xu, X. D.; Chen, C. S.; Cheng, S. X.; Zhang, X. Z.; Zhuo, R. X. *Macromol. Rapid Commun.* **2008**, *29*, 1726−1731.
(29) Xu, X. D.; Chen, J. X.; Cheng, H.; Zhang, X. Z.; Zhuo, R. X. *Polym. Chem.* **2012**, *3*, 2479−2486.
(30) Reddy, S. T.; Swartz, M. A.; Hubbell, J. A. *Trends Immunol.* **2006**, *27*, 573−579.
(31) Bachmann, M. F.; Jennings, G. T. *Nat. Rev. Immunol.* **2010**, *10*, 787−796.
(32) Black, M.; Trent, A.; Kostenko, Y.; Lee, J. S.; Olive, C.; Tirrell, M. *Adv. Mater.* **2012**, *24*, 3845−3849.
(33) Giancotti, F. G.; Ruoslahti, E. *Science* **1999**, *285*, 1028−1032.
(34) Chen, J. X.; Wang, H. Y.; Quan, C. Y.; Xu, X. D.; Zhang, X. Z.; Zhuo, R. X. *Org. Biomol. Chem.* **2010**, *8*, 3142−3148.
(35) Chen, J. X.; Wang, H. Y.; Li, C.; Han, K.; Zhang, X. Z.; Zhuo, R. X. *Biomaterials* **2011**, *32*, 1678−1684.
(36) Chen, J. X.; Xu, X. D.; Yang, S.; Yang, J.; Zhuo, R. X.; Zhang, X. Z. *Macromol. Biosci.* **2013**, *13*, 84−92.
(37) Hatakeyama, H.; Akita, H.; Harashima, H. *Adv. Drug Delivery Rev.* **2011**, *63*, 152−160.
(38) Nakamura, T.; Akita, H.; Yamada, Y.; Hatakeyama, H.; Harashima, H. *Acc. Chem. Res.* **2012**, *45*, 1113−1121.
(39) Gao, Y.; Kuang, Y.; Guo, Z. F.; Guo, Z. H.; Krauss, I. J.; Xu, B. *J. Am. Chem. Soc.* **2009**, *131*, 13576−13577.
(40) Wang, H. M.; Yang, C. H.; Wang, L.; Kong, D. L.; Zhang, Y. J.; Yang, Z. M. *Chem. Commun.* **2011**, *47*, 4439−4441.
(41) Mao, L. N.; Wang, H. M.; Tan, M.; Ou, L. L.; Kong, D. L.; Yang, Z. M. *Chem. Commun.* **2012**, *48*, 395−397.
(42) Lin, R.; Cheetham, A. G.; Zhang, P. C.; Lin, Y. A.; Cui, H. G. *Chem. Commun.* **2013**, *49*, 4968−4970.
(43) Minotti, G.; Menna, P.; Salvatorelli, E.; Cairo, G.; Gianni, L. *Pharmacol. Rev.* **2004**, *56*, 185−229.
(44) Kalaria, D. R.; Sharma, G.; Beniwal, V.; Ravi Kumar, M. N. *Pharm. Res.* **2009**, *26*, 492−501.
(45) Southan, C. *Drug Discov. Today* **2001**, *6*, 681−688.
(46) Hedstrom, L. *Chem. Rev.* **2002**, *102*, 4501−4524.